American Society for Neurochemistry

ASN Neuro
Volume 14: 1–13

DOI: 10.1177/17590914211073381
journals.sagepub.com/home/asn
SAGE

Optimization of Long-Term Human iPSC-Derived Spinal Motor Neuron Culture Using a Dendritic Polyglycerol Amine-Based Substrate

Louise Thiry[1], Jean-Pierre Clément[1], Rainer Haag[2], Timothy E Kennedy[1], and Stefano Stifani[1]

Abstract

Human induced pluripotent stem cells (hiPSCs) derived from healthy and diseased individuals can give rise to many cell types, facilitating the study of mechanisms of development, human disease modeling, and early drug target validation. In this context, experimental model systems based on hiPSC-derived motor neurons (MNs) have been used to study MN diseases such as spinal muscular atrophy and amyotrophic lateral sclerosis. Modeling MN disease using hiPSC-based approaches requires culture conditions that can recapitulate in a dish the events underlying differentiation, maturation, aging, and death of MNs. Current hiPSC-derived MN-based applications are often hampered by limitations in our ability to monitor MN morphology, survival, and other functional properties over a prolonged timeframe, underscoring the need for improved long-term culture conditions. Here we describe a cytocompatible dendritic polyglycerol amine (dPGA) substrate-based method for prolonged culture of hiPSC-derived MNs. We provide evidence that MNs cultured on dPGA-coated dishes are more amenable to long-term study of cell viability, molecular identity, and spontaneous network electrophysiological activity. The present study has the potential to improve hiPSC-based studies of human MN biology and disease.

We describe the use of a new coating substrate providing improved conditions for long-term cultures of human iPSC-derived motor neurons, thus allowing evaluation of cell viability, molecular identity, spontaneous network electrophysiological activity, and single-cell RNA sequencing of mature motor neurons.

Keywords

Human iPSCs, spinal motor neurons, dendritic polyglycerol amine, multi-electrode array, single cell RNA sequencing

Received September 17, 2021; Revised December 14, 2021; Accepted for publication December 22, 2021

Introduction

A major goal when studying human neurodegenerative diseases is to generate, culture, and study human neuronal cells displaying disease-relevant phenotypes. The use of human induced pluripotent stem cell (hiPSC)-derived neurons is providing the opportunity to model a variety of neurodegenerative diseases, thus facilitating the development of new therapeutics. For instance, loss of motor neuron (MN) functions is associated with several devastating neurodegenerative diseases including spinal muscular atrophy and amyotrophic lateral sclerosis (ALS) (Kanning et al., 2010; Nijssen et al., 2017). Several protocols exist to obtain MNs from hiPSCs (*e.g.*, Li et al., 2005; Amoroso et al., 2013; Qu et al., 2014; Du et al., 2015), and these cells have been used to study the pathophysiology of MNs from ALS and spinal muscular atrophy patients (*e.g.*, Ebert et al., 2009; Egawa et al., 2012; Chen et al., 2014; Kiskinis et al., 2014).

An important goal of MN disease modeling using hiPSCs is to implement culture conditions that can faithfully

[1]Department of Neurology and Neurosurgery, Montreal Neurological Institute-Hospital, McGill University, Montreal, Canada
[2]Institute of Chemistry and Biochemistry, Freie Universität Berlin, Berlin, Germany

Corresponding Author:
Stefano Stifani, Department of Neurology and Neurosurgery, Montreal Neurological Institute-Hospital, McGill University, 3801, rue University, Montreal (Quebec) H3A 2B4, Canada.
Email: stefano.stifani@mcgill.ca

recapitulate in a dish the processes underlying MN degeneration. This objective requires the ability to monitor molecular and functional properties of MNs, such as gene/protein expression, morphology, and electrical activity, in long-term cultures of MNs "aged" *in vitro*. However, prolonged culture of hiPSC-derived MNs is challenging with most commonly used MN derivation protocols. Most notably, hiPSC-derived MNs typically coalesce into large cell aggregates, and eventually detach from their substrate after continued culture, thus making long-term studies technically challenging (Kuijlaars et al., 2016; Taga et al., 2019; Thiry et al., 2020). Studies relying on endpoint assays requiring immunocytochemical staining, electrophysiological recordings of networks with multi-electrode array (MEA) devices, or single cell RNA sequencing (scRNAseq) applications are hindered by the presence of these large MN clusters, highlighting a critical need to develop improved hiPSC-derived MN culture conditions that would address these limitations and facilitate long-term studies.

Here we describe the use of a dendritic polyglycerol amine reagent (Hellmund et al., 2014; 2015) as a new coating substrate providing improved cytocompatible conditions for long-term cultures of hiPSC-derived MNs, thus allowing continued evaluation of cell viability, molecular identity, and spontaneous network electrophysiological activity. These culture conditions also facilitate scRNAseq studies of mature MNs due to decreased proportions of damaged cells when compared to more conventional coating protocols. These results demonstrate the value of using a dendritic polyglycerol amine substrate for real-time, long-term qualitative and quantitative analysis of hiPSC-derived MN cultures.

Materials and Methods

dPGA Substrate Synthesis and Application

Dendritic polyglycerol amine (dPGA: ~95 kDa, 50% amine content) (Hellmund et al., 2014; 2015) was synthetized, characterized, and applied to coverslips used for several different neuronal cultures as described in the accompanying manuscript by Clement and colleagues (Clement et al., submitted).

Generation of Motor Neurons from Human iPSCs

Human iPSC line NCRM-1 (male) was obtained from the National Institutes of Health Stem Cell Resource (Bethesda, MD, USA). Human iPSC line CS29iALS-C9n1.ISOxx, corresponding to a corrected, isogenic, line derived from a parental line generated from an ALS patient with *C9ORF72* gene mutation, was obtained from Cedars-Sinai (Los Angeles, CA, USA). Human iPSCs were differentiated into neural progenitor cells (NPCs), and subsequently MN progenitor cells (MNPCs) and MNs, as described previously (Thiry et al., 2020). After 24 days of differentiation, MNPCs were dissociated and plated at 50,000 cells/well on coverslips coated only with Matrigel (Thermo-Fisher Scientific; Cat. No. 08-774-552) or with dPGA plus Matrigel. For the latter condition, coverslips were coated with 300 µL/coverslip of a solution of PBS containing dPGA at varying concentrations (10, 25 or 50 µg/mL), and returned to the incubator for at least one hour before rinsing with PBS and coating with Matrigel on top of dPGA. MNs were differentiated in a chemically defined neural medium including DMEM/F12 supplemented with GlutaMAX (1/1; Thermo-Fisher Scientific; Cat. No. 35050-061), Neurobasal medium (1/1; Thermo-Fisher Scientific; Cat. No. 21103-049), N2 (0.5x; Thermo-Fisher Scientific; Cat. No. 17504-044), B27 (0.5x; Thermo-Fisher Scientific; Cat. No. 17502-048), ascorbic acid (100 µM; Sigma-Aldrich; Cat. No. A5960), antibiotic–antimycotic (1x; Thermo-Fisher Scientific; Cat. No. 15240-062), 0.5 µM retinoic acid, 0.1 µM purmorphamine, 0.1 µM Compound E (Calbiochem; Cat. No. 565790), insulin-like growth factor 1 (10 ng/mL; R&D Systems; Minneapolis, MN; Cat. No. 291-G1-200), brain-derived neurotrophic factor (10 ng/mL; Thermo-Fisher Scientific; Cat. No. PHC7074) and ciliary neurotrophic factor (10 ng/mL; R&D Systems; Cat. No. 257-NT-050). The MN culture medium was replaced every other day for 6 days and the MN cultures were characterized by immunocytochemistry as described below. For MEA recording, MNs were dissociated, plated at ~50,000 cells/well on Matrigel-coated or dPGA/Matrigel-coated wells of a CytoView MEA 24-well plate (Axion Biosystems; Atlanta, GA, USA; Cat. No. M384-tMEA-24 W), and cultured with the same MN medium described above. Culture medium was replaced every three days for one month, during which cells were recorded every week as described below.

Characterization of Human iPSC-Derived Cells by Immunocytochemistry

Immunocytochemical characterization of induced MNs was performed as described previously (Methot et al., 2018). The following primary antibodies were used: mouse anti-HOMEOBOX PROTEIN HB9 (HB9) (1/30; DSHB; Iowa City, IA, USA; Cat. No. 81.5C10-c); mouse anti-ISLET1 (ISL1) (1/30; DSHB; Cat. No. 39.4D5-c); rabbit anti-LIMB HOMEOBOX CONTAINING 3 (LHX3) (1/100; Abcam; Toronto, ON, Canada; Cat. No. ab14555); goat anti-FORKHEAD BOX PROTEIN 1 (FOXP1) (1/100; R&D Systems; Cat. No. AF4534); mouse anti-neurofilament protein (2H3) (1/35; DSHB; Cat. No. 2H3-c); and mouse anti-non-phosphorylated neurofilament H antibody SMI32 (1/100; BioLegend; San Diego, CA, USA; Cat. No. 801702). The indicated DSHB monoclonal antibodies were obtained from the Developmental Studies Hybridoma Bank, created by the NICHD of the NIH and maintained at The University of Iowa, Department of Biology, Iowa City, IA 52242. Secondary antibodies against primary reagents raised in various species were conjugated to Alexa Fluor 488,

Alexa Fluor 555, or Alexa Fluor 647 (1/1,000, Invitrogen; Burlington, ON, Canada). For quantification, images were acquired using an Axio Observer Z1 microscope connected to an AxioCam camera and using ZEN software (Zeiss). For each culture and each condition, images of >500 cells in 3 random fields were taken with a 20X objective and analyzed with Image J.

Multi-Electrode Array Recording of Human iPSC-Derived Motor Neuron Cultures

After 24 days of differentiation, hiPSC-derived MNs were plated at ~50,000 cells/well on Matrigel-coated or dPGA/Matrigel-coated wells of CytoView MEA 24-well plates (Axion Biosystems). Recordings from 16 electrodes per well were conducted using a Maestro (Axion BioSystems) MEA recording amplifier with a head stage maintaining a temperature of 32°C at 5% CO2. MEA plates were allowed to equilibrate for ~3 min prior to the 5 min recording of spontaneous activity. Data were sampled at 12.5 kHz, digitized, and analyzed using Axion Integrated Studio software (Axion BioSystems) with a band-pass filter (200–5000 Hz). The spontaneous electrophysiological activity of the hiPSC-derived cells was recorded every 7 days post-plating for 3 weeks: at day-32 (one-week post-plating), day-39 (two weeks post-plating), and day-46 (three weeks post-plating). The following electrophysiological parameters were analyzed: percentage of active electrodes, spike frequency, and firing rate.

Preparation of Single-Cells Suspensions

Suspensions of single cells were prepared from MNs cultured for 39 days (day 0 defined as start of NPC induction), approximately 2 weeks post-plating on either Matrigel only or dPGA (50 µg/mL)/Matrigel, as previously described (Thiry et al., 2020). Cells were counted to evaluate cell concentration and viability before scRNAseq.

Single Cell RNA Sequencing

Cells were sequenced on a single-cell level using the microdroplet-based protocol 10X Genomics Chromium Single Cell 3′ Solution, followed by Illumina sequencing at the McGill and Genome Quebec Innovation Center (https://cesgq.com/en-services). The 10X cDNA libraries were sequenced at a depth of 50,000 reads per cell on a HiSeq4000 system (Illumina).

In Silico Analysis

The raw scRNAseq data were first processed using the 10X pipeline (Cell Ranger) to demultiplex and align the sequences to the version GRCh38 of the human genome. The gene/cell matrices produced by Cell Ranger were used in the quality control processing and analysis. All the subsequent data analysis was conducted in R version 3.5.2 using Bioconductor Software Version 3.8. All packages are publicly available at the Bioconductor project (http://bioconductor.org). The workflow used for the analysis was adapted from a workflow previously developed to characterize hiPSC-derived MNs (Thiry et al., 2020) adapted from a published workflow designed to accommodate droplet-based systems such as 10X Chromium (Lun et al., 2016). Gene ontology analysis was performed on the 500 most up- or down-regulated genes between the two conditions using the web-based functional annotation tool DAVID (https://david.ncifcrf.gov/), as previously described (Huang et al., 2009).

Statistics

To detect differences in the proportion of total MNs, lateral motor column (LMC) MNs, or median motor column (MMC) MNs according to the substrate used for coating (i.e.; Matrigel alone or Matrigel in combination with either 10 µg/mL dPGA, 25 µg/mL dPGA, or 50 µg/mL dPGA), nonparametric Friedman test and Dunn's multiple comparisons post hoc test were used, because the variables did not fit a normal distribution (assessed by Kolmogorov-Smirnov test). Kruskal-Wallis and Dunn's multiple comparisons post hoc test was used to detect differences in the number of single-cells remaining attached to the coverslips after one-week post-plating, according to the substrate used for coating (same as above). Two-way ANOVA and Tukey's multiple comparison post hoc test were used to detect differences in the percentages of single-cells remaining attached to the coverslips at different time-points (one-, two- and three-weeks post-plating) according to the substrate used for the coating (i.e.; Matrigel alone or Matrigel and either 10 µg/mL dPGA, 25 µg/mL dPGA, or 50 µg/mL dPGA). The statistical significance was set at $p < 0.05$.

Results

Differentiation of Human iPSC-Derived Motor Neurons Cultured on dPGA/Matrigel

Spinal MNPCs and MNs were generated from the hiPSC NCRM-1 line as described previously (Thiry et al., 2020). While no single marker is completely MN-specific, spinal MNs are commonly characterized by transient co-expression of the LIM homeodomain transcription factors HB9 and ISL1/2 (Arber et al., 1999; Thaler et al., 1999) and most MN derivation studies rely on a combination of HB9 and ISL1 immunostaining (referred to as 'pan-MN' marker) (Amoroso et al., 2013) to characterize the MN phenotype *in vitro*. After 25 days of differentiation using standard culture conditions, 64% ± 6% of induced cells were pan-MN marker-positive (eg, ISL1/HB9-positive) (Figure 1A and 1C; "Matrigel"). A large proportion of the hiPSC-derived $ISL1^{+}/HB9^{+}$ MNs (48% ± 9%) expressed FOXP1, a known

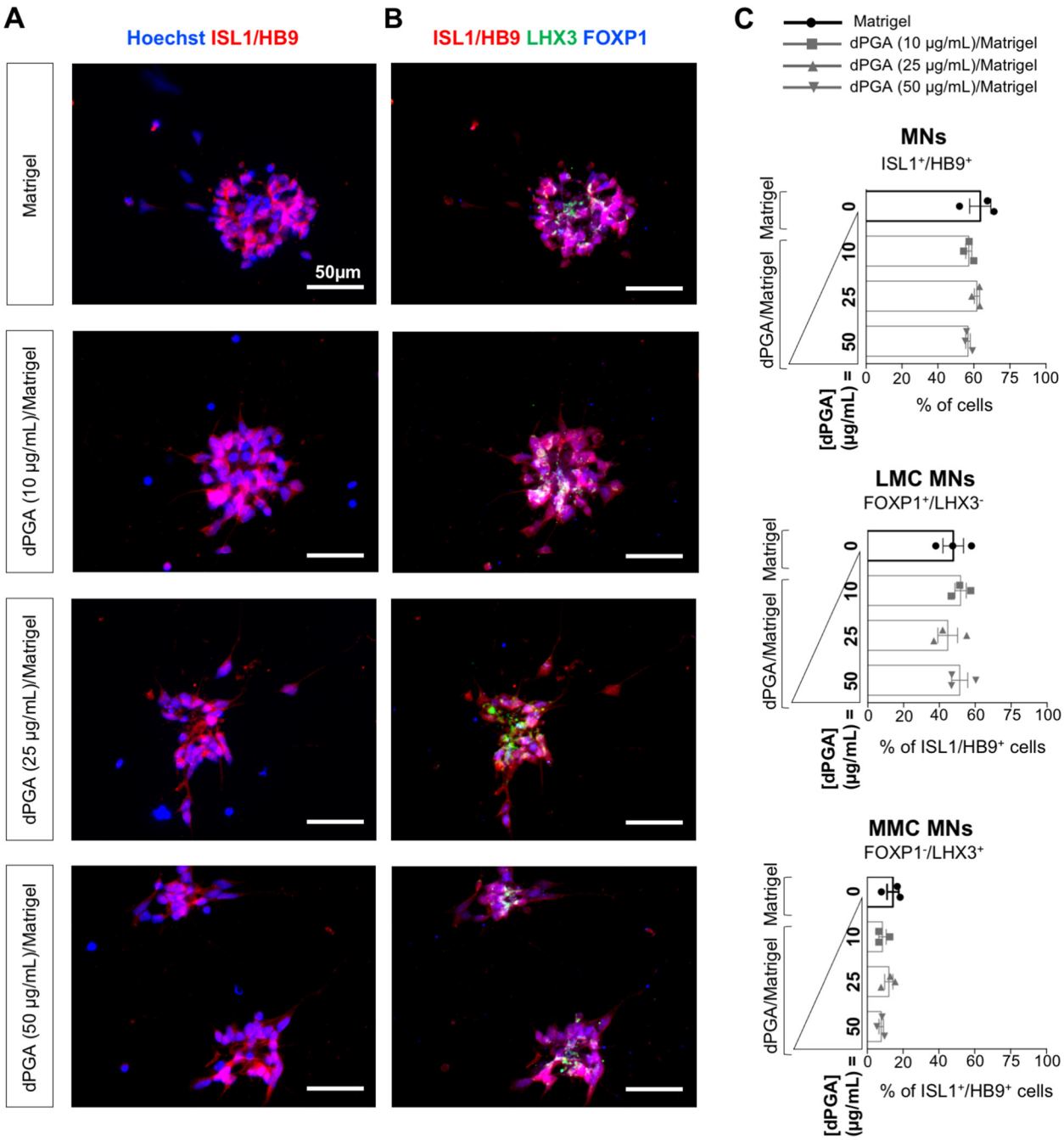

Figure 1. Efficient differentiation of hiPSCs into spinal motor neurons on dPGA/matrigel substrate. A-B) Representative images of MNs plated on Matrigel only vs dPGA (10, 25 or 50 µg/mL) and Matrigel combined, and co-stained with the known pan-MN marker ISL1/HB9 (red) **(A)**, as well as with anti-LHX3 (green) and anti-FOXP1 (blue) antibodies **(B),** after 25 days of culture. **C)** Quantification of all MNs (identified as $ISL1^+/HB9^+$), LMC MNs (identified as $ISL1^+/HB9^+/FOXP1^+/LHX3^-$), and MMC MNs (identified as $ISL1^+/HB9^+/LHX3^+/FOXP1^-$). MNs: 64% ± 6% for Matrigel, 57% ± 3% for dPGA10, 62% ± 3% for dPGA25 and 57% ± 2% for dPGA50; LMC MNs: 48% ± 9% for Matrigel, 52% ± 5% for dPGA10, 45% ± 9% for dPGA25 and 51% ± 8% for dPGA50; MMC MNs: 14% ± 6% for Matrigel, 9% ± 4% for dPGA10, 12% ± 4% for dPGA25 and 8% ± 3% for dPGA50. Scale bars, 50 µm. n = 3 cultures/condition (with >500 cells in 3 random fields for each culture). Friedman test and Dunn's multiple comparisons post hoc test. All p values are >0.05, i.e., not statistically significant. Data are shown as mean ± SEM. MMC, median motor column; LMC, lateral motor column.

marker of limb innervating MNs of the LMC (Dasen et al., 2003 and 2008; Amoroso et al., 2013) and did not express LHX3 (Thaler et al., 2002; Agalliu et al., 2009), thus exhibiting the typical LMC MN molecular profile ($FOXP1^+/LHX3^-$) (Figure 1B; top row; "Matrigel"; and Figure 1C; "LMC"). In contrast, only 14% ± 6% of the

hiPSC-derived MNs were FOXP1$^-$ and expressed LHX3, corresponding to the molecular profile (LHX3$^+$/FOXP1$^-$) of MNs of the MMC (Figure 1B; top row; "Matrigel"; and Figure 1C; "MMC").

Our work and that of others has previously shown that hiPSC-derived MNs usually coalesce into large cell clusters, which gradually detach from the culture device (Kuijlaars et al., 2016; Taga et al., 2019; Thiry et al., 2020). This situation is most likely due to the degradation of the protein-based substrate (Matrigel or laminin) commonly used for coating, a process that can be mediated by enzymes secreted by the cells (reviewed in Schmidt et al., 2018; Clement et al., submitted). To address this shortcoming, we sought to test the effect of a non-peptide polymer substrate, dPGA, that was shown to improve primary neuron culture conditions, possibly due to its resistance to degradation by cell-secreted proteases (Clement et al., submitted).

We first asked whether the use of the dPGA compound as a coating substrate in combination with Matrigel would affect the differentiation of hiPSCs into MNs. Cells were plated on either Matrigel-coated or dPGA/Matrigel-coated coverslips, with varying concentrations of dPGA (10, 25 or 50 µg/mL), followed by immunocytochemistry after 25 days of culture (Figure 1). A similar proportion (~60%) of the cells plated on Matrigel only or dPGA/Matrigel expressed the pan-MN marker ISL1/HB9 (Figure 1C). Furthermore, no statistically significant difference was found in the proportion of FOXP1$^+$/LHX3$^-$ LMC MNs and FOXP1$^-$/LHX3$^+$ MMC MNs present in the cultures grown on either Matrigel only or dPGA/Matrigel, regardless of the concentration of dPGA used (Figure 1C).

Together, these observations show that the dPGA coating does not detectably interfere with the differentiation of hiPSCs into MNs, suggesting that it can be used for the culture of hiPSC-derived MNs.

Improved Long-Term Culture of Human iPSC-Derived Motor Neurons on dPGA/Matrigel

To test whether a dPGA coating would enhance long-term culture of hiPSC-derived MNs, we analyzed induced cultures up to three-weeks post-plating. As early as one-week post-plating on Matrigel only (i.e.; 32 days (D32) after the start of the differentiation protocol), hiPSC-derived MNs coalesced into large cell clusters, with their cell bodies crowded into clumps and their processes hyper-fasciculated into well-defined bundles (Figure 2A). In contrast, at the same time-point, hiPSC-derived MNs plated on dPGA/Matrigel remained more homogeneously distributed over the coverslip, with their processes creating widespread arborizations, regardless of the three tested dPGA concentrations (Figure 2B-D). The number of single cells remaining attached to the coverslip was systematically increased by the use of the dPGA substrate (Figure 2E). Interestingly, this effect appeared to be proportional to the concentration of dPGA used, with 10 µg/mL leading to a 4.7 ± 2.7-fold increase, 25 µg/mL leading to a 5.3 ± 1.8-fold increase and 50 µg/mL leading to a 7 ± 2-fold increase in the number of single-cells. Only the use of dPGA at 50 µg/mL led to a statistically significant effect, suggesting that this concentration is the most effective to improve hiPSC-derived MN culture conditions.

To evaluate whether this effect of the dPGA coating was stable over time, we next compared the percentages of cells remaining attached to Matrigel- or dPGA/Matrigel-coated coverslips after one week, two weeks and three weeks post-plating (Figure 2F). Both the type of coating substrate (e.g., Matrigel only vs. dPGA/Matrigel) and the culture time significantly affected cell adherence to the coverslips. As early as one-week post-plating, less than 10% of the cells plated on Matrigel-coated coverslips remained attached and this number decreased over time with all cells becoming detached at three weeks post-plating (Figure 2F, black line). In contrast, a minimum of 50% of the cells plated on dPGA/Matrigel-coated coverslips remained attached over-time, even three weeks after plating (Figure 2F, grey lines) ($p < 0.0001$; Two-way ANOVA). This effect was proportional to the concentration of dPGA used, although each of the three tested concentrations led to a statistically significant increased adherence when compared to Matrigel only. A dPGA concentration of 10 µg/mL was significantly less efficient than 25 or 50 µg/mL, and there was no statistical difference between the effect obtained with a dPGA concentration of 25 or 50 µg/mL. As shown in Figure 2G-H, MNs grown on dPGA (50 µg/mL)/Matrigel could be maintained in culture for at least 2-months post-plating without clumping, and they remained scattered over the coverslip and created widespread arborizations with their processes.

To confirm and extend these observations, MNs were derived from a separate human iPSC line (CS29iALS-C9n1.ISOxx), cultured for three weeks, and subjected to immunocytochemistry with a non-phosphorylated neurofilament protein (SMI-32) antibody, which is routinely used to mark MNs (Tsang et al., 2000). Human iPSC-derived MNs remained homogeneously distributed over the coverslips, with widespread arborizations of their processes, three weeks after plating on dPGA (50 µg/mL)/Matrigel (Figure 2I). An average of 79% ± 10% of the cells remained attached to the coverslip (Figure 2J), allowing quantitative analysis of day-46 cultures, which revealed that 60% ± 4% of the cells were SMI32$^+$ mature MNs (Figure 2 K).

Together, these results provide evidence that using the dPGA substrate in conjunction with Matrigel improves the long-term culture conditions of MNs, allowing real-time, long-term qualitative and quantitative analysis of these cells.

Long-Term Multielectrode Array Recordings of Human iPSC-Derived Motor Neurons Cultured on dPGA/Matrigel

Electrophysiological characterization of hiPSC-derived MNs is crucial to assess their function. Multielectrode arrays are

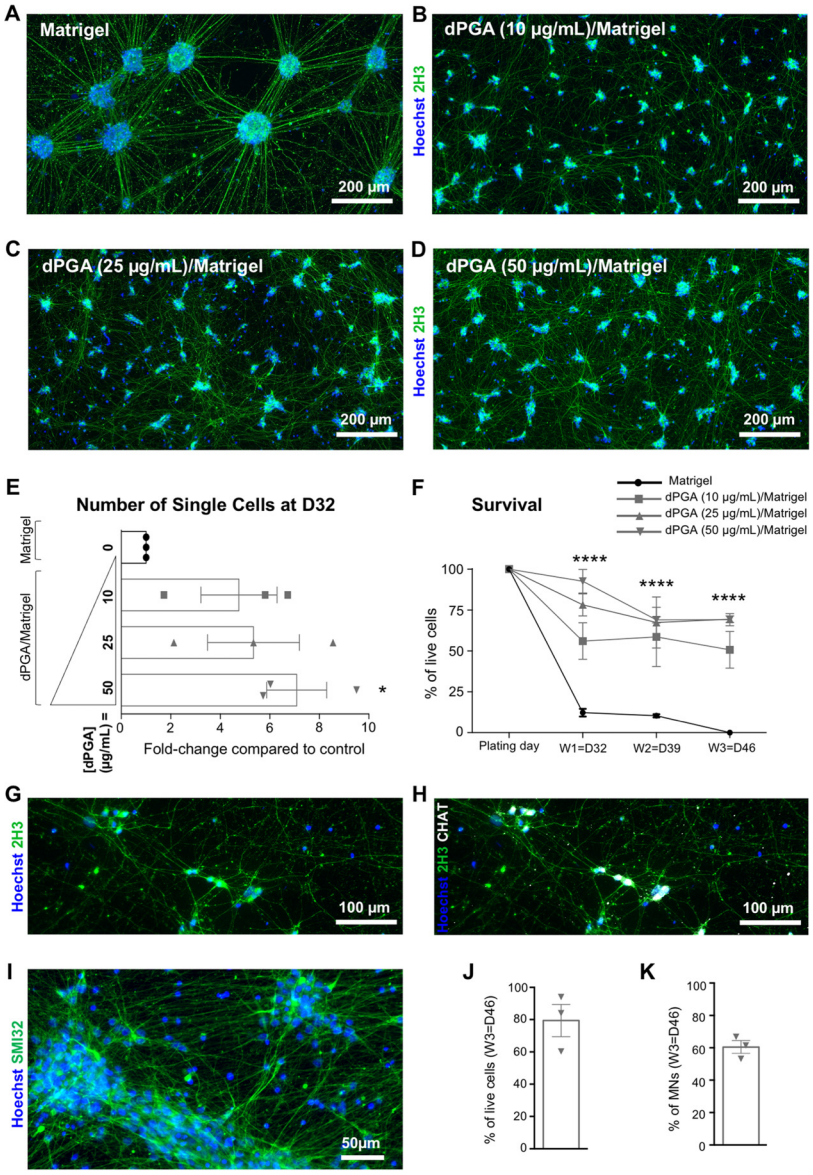

Figure 2. Enhanced long-term culture of human iPSC-derived motor neurons on dPGA/matrigel substrate. A-D) Representative images of NCRM1 hiPSC line-derived MNs one-week post-plating (i.e., 32 days of differentiation) on either Matrigel only **(A)**, dPGA (10 µg/mL)/Matrigel **(B)**, dPGA (25 µg/mL)/Matrigel **(C)**, or dPGA (50 µg/mL)/Matrigel **(D)**, and stained with Hoechst (blue) and the anti-neurofilament 2H3 antibody (green). Scale bars, 200 µm. **E)** Fold change of the number of single cells counted one-week post-plating (i.e., 32 days of differentiation) on either Matrigel only (black) or dPGA/Matrigel (grey). n = 3 cultures/condition (with 3 random fields for each culture); *, $p < 0.05$; Kruskal-Wallis and Dunn's multiple comparisons post hoc test. **F)** Cell number curves from cultures plated on Matrigel only vs dPGA/Matrigel showing the percentages of cells remaining attached to the coverslip after one (i.e., 32 days of differentiation), two (i.e., 39 days) and three (i.e., 46 days) weeks post-plating, as compared to the number of cells plated (100%) (n = 5 cultures/condition). Both factors (substrate and time) significantly affected cell adherence to the coverslips ($p < 0.0001$; Two-way ANOVA), and Tukey's multiple comparisons post hoc tests revealed a statistically significant improvement with dPGA (10, 25, or 50 g/mL)/Matrigel compared to Matrigel only (****, $p < 0.0001$). Furthermore, dPGA concentrations of 25 and 50 µg/mL were statistically significantly more efficient then dPGA (10 µg/mL) ($p < 0.05$), while dPGA (25 µg/mL) vs dPGA (50 µg/mL) was not significantly different (Tukey's multiple comparisons post hoc tests). Data are shown as mean ± SEM. **G, H)** Representative images of NCRM1 hiPSC line-derived MNs two-months post-plating (i.e., 81 days of differentiation) on dPGA (50 µg/mL)/Matrigel: cells were stained with Hoechst (blue) and anti-neurofilament antibody 2H3 (green) **(G)**, or with Hoechst (blue), anti-neurofilament antibody 2H3 (green) and MN marker anti-CHAT antibody (white) **(H)**. Scale bars, 100 µm. **I)** Representative image of CS29iALS-C9n1.ISOxx hiPSC line-derived MNs stained with Hoechst (blue) and the MN marker anti-SMI32 antibody (green) after three weeks post-plating (i.e. 46 days of differentiation) on dPGA (50 µg/mL) /Matrigel. Scale bars = 50 µm. **J)** Percentages of cells remaining attached to the coverslip three weeks post-plating, as compared to the number of cells plated (100%). **K)** Proportion of SMI32 + MNs three weeks post-plating. Data are shown as mean ± SEM. n = 3 cultures, with 3 random fields for each culture.

particularly suited for this purpose as they enable the recording of large neuronal populations through the detection of extracellular voltages. As reported by others (Kuijlaars et al., 2016; Taga et al., 2019), we observed that hiPSC-derived MNs plated on Matrigel-coated MEA wells formed large cell aggregates (Figure 3A). This made it difficult to record the electrophysiological activity of these cells, as reflected by a low number of electrodes with persistent activity during the three-week recording period (Figure 3C, black line). To test whether the use of dPGA/Matrigel coating could improve MEA analysis of hiPSC-derived MNs, we recorded hiPSC-derived MNs plated on either Matrigel- or dPGA/Matrigel-coated MEA plates, with varying concentrations of dPGA (10, 25 or 50 µg/mL), over a three-week period after plating (Figure 3). In contrast to the hiPSC-derived MNs plated on Matrigel alone, which coalesced into large cell clusters as early as one-week post-plating (Figure 3A), hiPSC-derived MNs plated on dPGA/Matrigel remained evenly distributed on the MEA wells (Figure 3B). As a result, each of the 16 electrodes in each of the dPGA/Matrigel-coated wells remained in the immediate vicinity of a number of cells for the three-week recording periods. This observation was reflected by a statistically significant increase in the number of electrodes with persistent activity over these recording periods in dPGA/Matrigel-coated wells (Figure 3C, grey lines) as compared to Matrigel-coated wells (Figure 3C, black line). This effect was consistent across the three tested concentrations of the dPGA substrate, without statistical difference between each concentration. Consequently, over the three-week recording periods, both the number of spikes (Figure 3D) and the mean firing rate (Figure 3E) were statistically significantly increased in dPGA/Matrigel-coated wells (grey lines) as compared to Matrigel-coated ones (black line). Together, these results suggest that using the dPGA substrate in combination with Matrigel enables stable long-term MEA recordings of hiPSC-derived MNs.

Long Term Cultures of Human iPSC-Derived Motor Neurons on dPGA/Matrigel for Single-Cell RNA Sequencing

Microdroplet-based scRNAseq analysis provides a powerful tool to validate the quality and composition of hiPSC-derived MN cultures by enabling a precise characterization of the genome-wide expression profile of individual cells (Stegle et al., 2015; Thiry et al., 2020). As shown above, induced MNs already begin to coalesce into large cell clusters as early as one-week post-plating on Matrigel, making it challenging to perform scRNAseq studies due to the difficulty of isolating viable single cells. To address this situation, we evaluated whether the use of dPGA/Matrigel coating, which leads to reduced MN clustering, would facilitate the application of scRNAseq to the study of hiPSC-derived MNs. We submitted hiPSC-derived MNs plated on either Matrigel only ("Matrigel") or 50 µg/mL dPGA/Matrigel ("dPGA/Matrigel") to scRNAseq at 39 days of differentiation. After transcriptomic data (FASTQ files) were acquired from ~6000 single cells for each sample, we used the Bioconductor software (Lun et al., 2016) to perform quality control (QC) steps to filter out damaged cells (Figure 4A to C). A total of 4375 cells of the "Matrigel" sample and 5857 cells of the "dPGA/Matrigel" sample passed QC. Interestingly, the median number of mapped reads per cell was lower in Matrigel as compared to dPGA/Matrigel conditions [Figure 4A; 6369 for Matrigel (top) and 9302 for dPGA/Matrigel (bottom)]. Similarly, the median number of genes expressed per cell was lower in Matrigel as compared to dPGA/Matrigel conditions [Figure 4B; 2685 for Matrigel (top) and 3168 for dPGA/Matrigel (bottom)]. Together, these QC metrics suggest a reduced proportion of damaged cells (i.e., the cells with lower numbers of detected genes and mapped reads) in the "dPGA/Matrigel" sample compared to "Matrigel". In addition, the percentage of mitochondrial genes present in most cells was higher in Matrigel" compared to "dPGA/Matrigel" samples [Figure 4C; 10.3% for Matrigel (top) and 8.7% for dPGA/Matrigel (bottom)], suggesting a high proportion of damaged cells and/or debris in both samples, but in a reduced proportion in the "dPGA/Matrigel" sample, compared to "Matrigel".

After QC, the remaining cells were submitted to principal-component analysis and t-distributed stochastic neighbor embedding (t-SNE) analysis (Figure 4D). In both samples, a large number of damaged/dying cells were identified, based on their low QC metrics and/or their high levels of expression of known markers of cell death such as *BCL2*, *BAX*, *NGF, BOK, ATM, PSEN1, RB1, LIG4, CDK5, PARP1, BAD, MAP3K11, UBE2 M* (Wei et al., 2001, D'Orsi et al., 2015; Frade & Barde, 1999) (Figure 4E). To further characterize this situation, we next performed integrative analysis to compare the cell proportions and gene expression differences between "Matrigel" (Figure 4F) and "dPGA/Matrigel" (Figure 4G) samples. Although a large proportion of cells were identified as "damaged cells" in both samples, this fraction was markedly reduced in the "dPGA/Matrigel" sample (47%; Figure 4G) as compared to "Matrigel" (70%; Figure 4F). Consequently, a larger proportion of cells were identified either as MNs and MNPCs ("MNs"; 16% in dPGA/Matrigel vs. 10% in Matrigel) based on their expression of the specific markers NEUROGENIN2 (*NEUROG2*), *OLIG2, HB9, ISL1, ISL2* and CHOLINE ACETYL TRANSFERASE (*CHAT*), or as interneurons ("INs"; 28% in dPGA/Matrigel vs. 12% in Matrigel) based on their expression of the specific markers *PAX2*, *PAX3*, *LBX1*, *EVX1*, *EN1*, *CHX10*, *GATA3*, *SOX14*, *SIM1*, *TLX3*. Of note, other cell types were identified in relatively comparable proportions in both samples: oligodendrocytes accounted for approximately 7% of the cells in "Matrigel" and 9% in "dPGA/Matrigel",

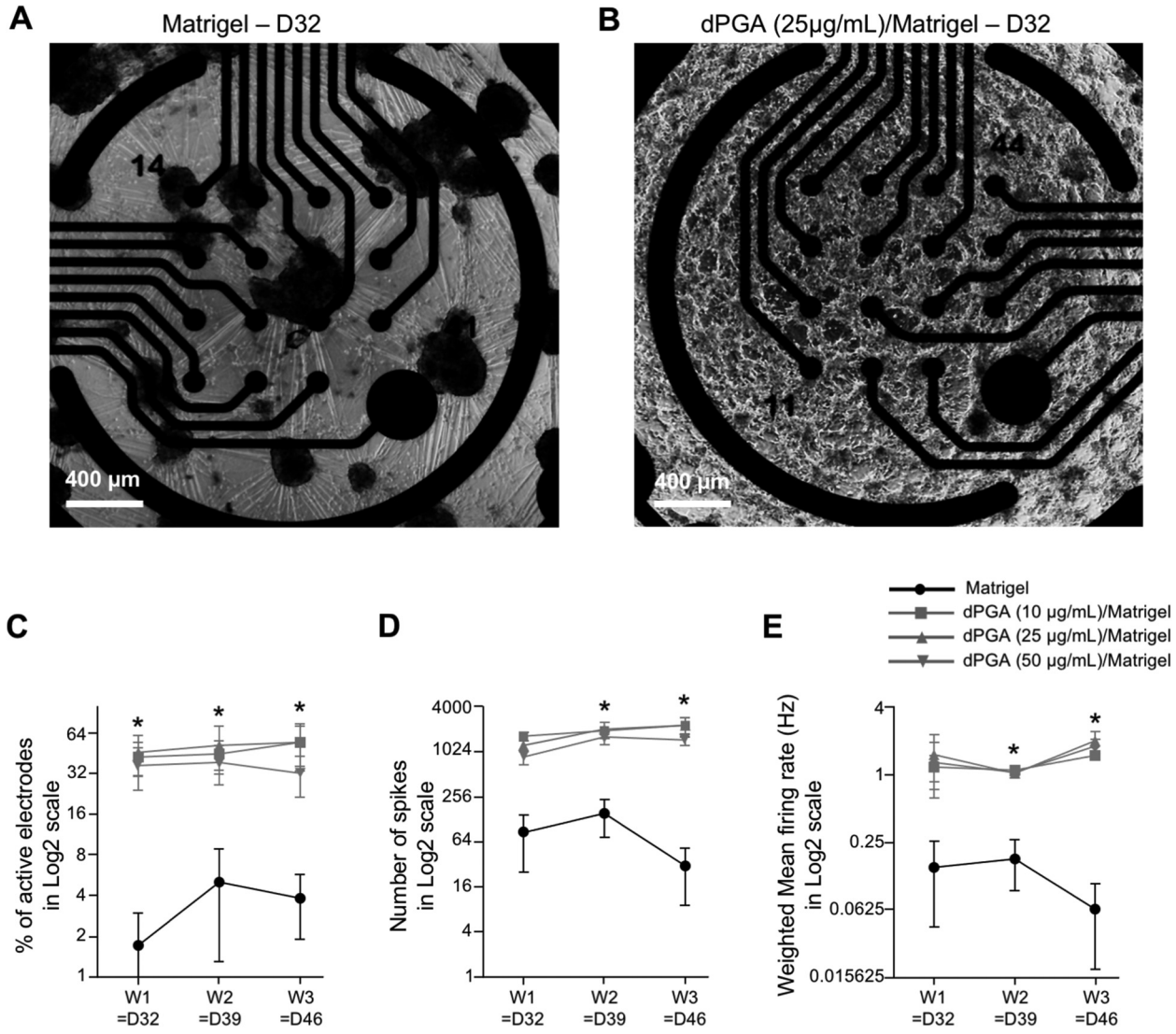

Figure 3. The dPGA/matrigel substrate enables long-term multielectrode array recordings of human iPSC-derived motor neurons. A-B) Representative images of hiPSC-derived MNs one-week post-plating (i.e., 32 days of differentiation) on MEA wells coated with either Matrigel only **(A)** or dPGA (25 µg/mL)/Matrigel **(B)**. Scale bars, 400 µm. **C-E)** Percentage of active electrodes **(C)**, number of spikes **(D),** and weighted mean firing rate (Hz) **(E)** of MN cultures plated on Matrigel only vs dPGA (10, 25, or 50 µg/mL)/Matrigel at one (W1)-, two) (W2- and three-weeks (W3) post-plating. (**C**) The percentage of active electrodes was significantly increased with dPGA (10, 25, or 50 g/mL)/Matrigel compared to Matrigel ($p < 0.0001$; Two-way ANOVA): Tukey's multiple comparisons post hoc tests further revealed a statistically significant improvement with dPGA (10, 25, or 50 g/mL)/Matrigel compared to Matrigel only at W1, W2 and W3 post-plating (*, $p < 0.05$). There was no statistically significant difference between the various concentration of dPGA (Tukey's multiple comparisons post hoc tests). (**D, E**) The substrate significantly affected the number of spikes ($p = 0.0016$; Two-way ANOVA) (**D**), and the weighted mean firing rate ($p = 0.0015$; Two-way ANOVA) (**E**). Furthermore, Tukey's multiple comparisons post hoc tests revealed a statistically significant improvement with dPGA (10, 25, or 50 g/mL)/Matrigel compared to Matrigel only at W2 and W3 post-plating (*, $p < 0.05$) for both the number of spikes (**D**) and the weighted mean firing rate (**E**), while there was no statistically significant difference between the various concentration of dPGA. $n = 3$ cultures, with 6 wells for each culture. Data are shown as mean ± SEM on Log2 scales.

while undifferentiated cells (iPSCs), NPCs and astrocytes were almost absent in both samples, as expected. Importantly, functional analysis of the most differentially expressed genes between the two culture conditions revealed a significant enrichment in Gene Ontology 'Biological Processes' terms related to apoptosis and the negative regulation of cell adhesion in the 500 most down-regulated genes in "dPGA/Matrigel". In comparison, terms related to the regulation of transcription/translation were significantly enriched in 500 most up-regulated genes in the "dPGA/Matrigel" sample (Supplemental Figure 1).

Together, these scRNAseq results show that although it is technically challenging to isolate single MNs from 'more mature' hiPSC-derived cultures without causing cell damage

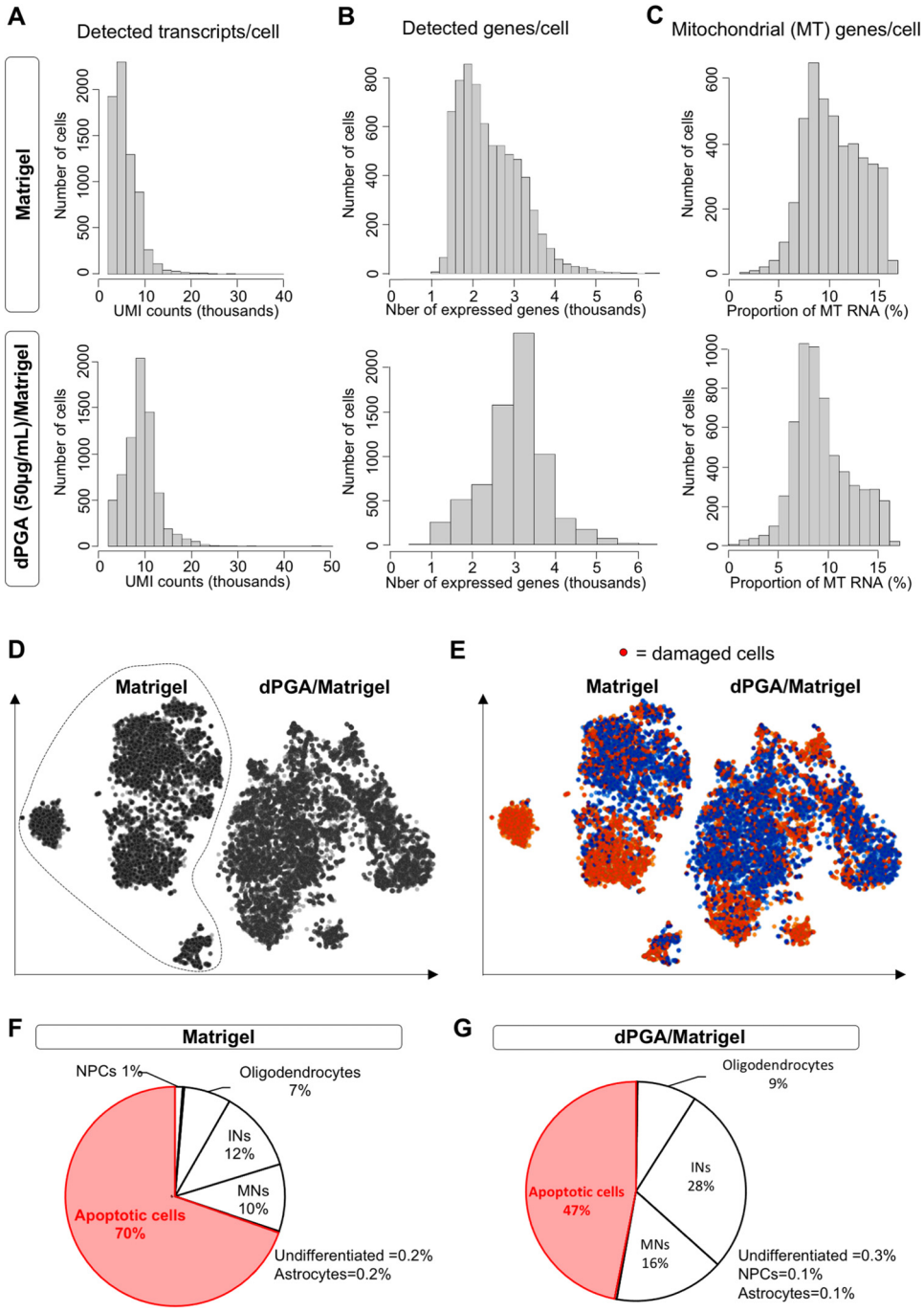

Figure 4. Reduced proportion of damaged cells after single cell RNA sequencing analysis of human iPSC-derived motor neuron cultures grown on dPGA/matrigel. A-C) Quality control metrics for hiPSC-derived MN cultures grown on either Matrigel only (top graphs) or dPGA (50 µg/mL)/Matrigel (bottom graphs) after 39 days of differentiation, with the number of detected transcripts per cell (**A**), the number of detected genes per cell (**B**), and the number of mitochondrial (MT) genes per cell (**C**) depicted. **D**) t-SNE plot of hiPSC derived MN cultures grown on either Matrigel only (circled area) or dPGA (50 µg/mL)/Matrigel after 39 days of differentiation. Each dot corresponds to a cell. **E**) t-SNE plot of the same hiPSC-derived MN cultures as in D), colored in red for cells identified as damaged (based on low QC metrics and/or expression of known apoptotic markers such as *BCL2*, *BAX*, *NGF, BOK, ATM, PSEN1, RB1, LIG4, CDK5, PARP1, BAD, MAP3K11, UBE2 M*). F-G) Relative proportion of undifferentiated cells, NPCs, interneurons (INs), MNs, astrocytes, oligodendrocytes, and damaged cells, identified two weeks post-plating (i.e.; 39 days of differentiation) on either Matrigel only (**F**) or dPGA (50 µg/mL)/Matrigel (**G**), based on their level of expression of the following genes: *NANOG* and *OCT4* for undifferentiated cells; *SOX1*, *SOX2*, and *MKI67* for NPCs; *PAX2*, *PAX3*, *LBX1*, *EVX1*, *EN1*, *CHX10*, *GATA3*, *SOX14*, *SIM1*, *TLX3* for INs; *NEUROG2*, *OLIG2*, *HB9*, *ISL1*, *ISL2*, *CHAT* for MNs; *S100B and SOX9* for astrocytic glial cells; *PDGFRα* and *GALC* for oligodendrocytes; *BCL2*, *BAX*, *NGF, BOK, ATM, PSEN1, RB1, LIG4, CDK5, PARP1, BAD, MAP3K11, UBE2 M* for apoptotic cells.

in the process, the quality of single-cell suspensions for scRNAseq can be significantly improved by the use of dPGA/Matrigel coating during the maturation of hiPSC-derived MN cultures.

Discussion

Despite rapid advancements in iPSC-based technologies, current neuronal differentiation protocols tend to generate cells with properties of relatively immature neurons. This poses a problem when using iPSC-derived neurons to model age-related pathologies, including ALS (Arbab et al., 2014; Luisier et al., 2018; Mertens et al., 2015; Miller et al., 2013; Patani et al., 2012; Ho et al., 2016). Transcriptomic comparison of hiPSC-derived spinal MNs suggests that they are more similar to fetal than adult spinal cells (Ho et al., 2016; Luisier et al., 2018). Maturation- and age-related pathways are thought to play roles in MN disease pathology, highlighting the necessity to develop strategies to study '*in vitro* matured' hiPSC-derived MNs to provide more disease-relevant iPSC-based models of ALS. However, hiPSC-derived MN maturation is made difficult in most current derivation protocols by the appearance of large MN aggregates, often as early as 5-7 days post-plating, which cause significant cell loss and hinder the analysis of single cells (Kuijlaars et al., 2016; Taga et al., 2019; Thiry et al., 2020). This shortcoming underscores a critical need to improve long-term culture of hiPSC-derived MNs to increase the fractions of viable single cells. Based on these observations, the present study aimed at developing enhanced culture conditions to facilitate the study of cell viability, molecular identity, and network electrophysiological activity in long-term hiPSC-derived MNs.

The extracellular matrix (ECM) performs a number of important functions, including mediation of cell–cell interactions, cell adhesion and migration, control of cell proliferation and differentiation, and apoptosis (Kharkar et al., 2013; Wang & Heilshorn. 2015). Over the past decades, the development of artificial ECM materials, for example via the use of ECM-mimicking substrates like Matrigel, has allowed the *in vitro* expansion and differentiation of iPSCs in a controllable, robust and scalable manner (reviewed in Schmidt et al., 2018). However, such protein-based substrates are susceptible to degradation by enzymes secreted by the cells, impacting on their use for long-term culture. To overcome this situation, non-peptide polymer substrates that are resistant to enzymatic degradation by the cells, like the cytocompatible dPGA, can be used in combination with peptide-based substrates to achieve a balance between resistance to protein degradation and lack of inherent biological activity of synthetic polymers. The accompanying manuscript by Clement and colleagues (Clement et al., submitted) provides further information on dPGA synthesis, application to coversplips used for cultures of a variety of neuronal types, as well as structure of dPGA-coated surfaces. In the present study, we have provided evidence suggesting that the use of this approach has the potential to specifically improve the study of hiPSC-derived MNs, by enhancing morphological, immunocytochemical, and survival studies, extracellular electrophysiological recordings, and single-cell RNA sequencing.

Our results have shown that dPGA coating in conjunction with Matrigel does not interfere with the differentiation of hiPSCs into MNs. More importantly, it results in a more homogeneous distribution of hiPSC-derived MNs, with widespread arborizations of their processes after the first week post-plating. These improved conditions result in a significant increase in MN survival over time, when compared to coating without dPGA. This advancement is expected to allow improved long-term qualitative and quantitative morphological and immunocytochemical analysis, as well as survival studies, of more mature hiPSC-derived MNs. This progress will benefit MN disease research, and ALS research in particular, based on hiPSC-derived MNs in a number of ways. For instance, it will facilitate the study of how different subtypes of spinal MNs, differing in gene expression, connectivity and function (William et al., 2003), are specifically vulnerable to degeneration in ALS (Chakkalakal et al., 2010). Being able to identify each subtype present in more mature iPSC-derived MN cultures, and to monitor changes in the morphology and survival rate of each MN subtype, will provide insight into the mechanisms responsible for driving differential susceptibility to degeneration. More generally, a growing number of studies of immature MNs derived from ALS patient iPSCs have shown their potential in recapitulating early morphological and disease-relevant molecular phenotypes, including RNA foci, protein inclusions, neurofilament aggregation, nucleoplasmic transport disruption, and cell death (Sareen et al., 2013; Chen et al., 2014; Kiskinis et al., 2014; Zhang et al., 2015). However, it remains to be determined how these phenotypes contribute to disease progression in more mature MNs. The availability of experimentally tractable '*in vitro* matured' cultures will provide better model systems to answer these questions.

Beyond morphological, immunocytochemical and survival studies, the electrophysiological characterization of hiPSC-derived MNs is crucial to obtain accurate measures of their function. Multielectrode arrays are particularly suited for electrophysiological studies as they enable the extracellular recording of large populations of neurons, allowing for extended recordings that are important for a number of objectives, including drug testing. As shown in this study, and previously observed by others (Kuijlaars et al., 2016; Taga et al., 2019), hiPSC-derived MNs plated on a peptide-based substrate typically form a significant number of large cell aggregates that make it difficult to discern specific synaptic connections between the cells and to record their electrophysiological activity. We have shown that the plating of hiPSC-derived MNs on dPGA/Matrigel coated-MEA plates results in a more homogeneous distribution of the cells and a greater number of electrodes showing persistent activity overtime. Such improved experimental conditions will enable the monitoring of the electrophysiological activity of hiPSC-derived MNs over extended periods of time, an important goal of ALS research. For instance, analysis

of MNs generated from *C9ORF72* patient-derived iPSCs revealed that these cells display an initial period of hyperexcitability followed by a progressive loss in action potential output and synaptic activity at later timepoints (Devlin et al., 2015). These temporal changes could explain why several studies reported divergent findings regarding the inherent excitability of ALS iPSC-derived MNs (Sareen et al., 2013; Wainger et al., 2014; Naujock et al., 2016). While electrophysiological changes are a major phenotype in iPSC-based models of ALS, whether hyper- or hypo-excitability plays a crucial role in the disease remains unclear, highlighting the need to investigate the electrophysiological properties of ALS iPSC-derived MNs over extended periods of time in a stable and scalable manner.

The study of hiPSC-derived MNs using scRNAseq becomes increasingly challenging as cultures mature *in vitro*, most likely due to the harsher conditions needed to dissociate larger MN clusters. In previous studies, we have shown that scRNAseq data obtained from relatively immature hiPSC-derived MNs (28 days of differentiation) identified approximately 4% of dying cells (Thiry et al., 2020). In contrast, the present studies have revealed that a significantly larger proportion of more mature cells (39 days after differentiation) were identified as damaged cells using scRNAseq. However, the proportion of damaged cells in hiPSC-derived MNs cultures subjected to scRNAseq at later timepoints can be significantly reduced by the use of the dPGA/Matrigel combination as a coating substrate. This finding is expected to facilitate future scRNAseq studies of more mature hiPSC-derived MN cultures, thus enabling gene expression profiling of cells more likely to provide information on phenotypes that may be more relevant to MN disease pathophysiology.

In summary, the present study provides evidence that dPGA coating improves experimental conditions for the long-term culture of hiPSC-derived MNs, resulting in a more homogeneous distribution of the somas and a widespread arborizations of their processes, as well as a significant increase in MN survival over time. These improved experimental conditions will facilitate the study of more mature hiPSC-derived MNs, by enabling a better application of cell imaging techniques, electrophysiological recordings, as well as scRNAseq approaches, all of which are heavily reliant on the quality of long-term MN cultures. In turn, improved long-term culture of hiPSC-derived MNs will facilitate the study of phenotypes associated with neurodegeneration, thus providing a more informative experimental model system to develop cellular assays and facilitate early-stage drug discovery efforts in ALS and other age-related MN diseases.

List of abbreviations used

dPGA	= dendritic polyglycerol amine
hiPSC	= human induced pluripotent stem cell
IN	= interneuron
LMC	= lateral motor column
MEA	= multielectrode array
MMC	= median motor column
MN	= motor neuron
NPC	= neural progenitor cell
scRNAseq	= single cell RNA sequencing

Acknowledgments

We thank Dr. Thomas Durcan for advice and for providing access to multielectrode array recording set-up, Dr. Ragoussis' team at the McGill University and Genome Quebec Innovation Center for scRNA library preparation, as well as Rita Lo for invaluable assistance. We also acknowledge Cathleen Schlesener and Markus Hellmund for their help in the dPGA synthesis.

Author Contributions

LT designed and performed all experiments, data analysis, figures and wrote the first draft of the manuscript. SS, LT, J-PC and TEK conceived the study plan. RH provided and validated the dPGA. SS supervised data analysis and manuscript writing.

Declaration of Conflicting Interests

The author(s) declared no potential conflicts of interest with respect to the research, authorship, and/or publication of this article.

Funding

The author(s) disclosed receipt of the following financial support for the research, authorship, and/or publication of this article: This work was supported by grants to S.S. from the Canadian Institutes for Health Research and Fonds de la recherche en Sante-Quebec under the frame of E-Rare-3, the ERA-Net for Research on Rare Diseases, and from the Avrith Neuro-Cambridge Neuroscience Collaboration Initiative. SS is a James McGill Professor of McGill University.

ORCID iDs

Timothy E Kennedy https://orcid.org/0000-0003-4454-5080
Stefano Stifani https://orcid.org/0000-0002-2376-7701

Supplemental material

Supplemental material for this article is available online.

References

Agalliu, D., Takada, S., Agalliu, I., McMahon, A. P., Jessell, T. M. (2009). Motor neurons with axial muscle projections specified by Wnt4/5 signaling. *Neuron*, *61*(5), 708–720. https://doi.org/10.1016/j.neuron.2008.12.026

Amoroso, M. W., Croft, G. F., Williams, D. J., O'Keeffe, S., Carrasco, M. A., Davis, A. R., Roybon, L., Oakley, D. H., Maniatis, T., Henderson, C. E., Wichterle, H. (2013). Accelerated high-yield generation of limb-innervating motor neurons from human stem cells. *J. Neurosci*, *33*(2), 574–586. https://doi.org/10.1523/JNEUROSCI.0906-12.2013

Arbab, M., Baars, S., Geijsen, N. (2014). Modeling motor neuron disease: The matter of time. *Trends in Neurosciences*, *37*(11), 642–652. https://doi.org/10.1016/j.tins.2014.07.008

Arber, S., Han, B., Mendelsohn, M., Smith, M., Jessell, T. M., Sockanathan, S. (1999). Requirement for the homeobox gene

Hb9 in the consolidation of motor neuron identity. *Neuron*, *23(4)*, 659–674. https://doi.org/10.1016/S0896-6273(01)80026-X

Chakkalakal, J. V., Nishimune, H., Ruas, J. L., Spiegelman, B. M., Sanes, J. R. (2010). Retrograde influence of muscle fibers on their innervation revealed by a novel marker for slow motoneurons. *Development (Cambridge, England)*, *137*(20), 3489–3499. https://doi.org/10.1242/dev.053348

Chen, H., Qian, K., Du, Z., Cao, J., Petersen, A., Liu, H., Blackbourn, L. W.4th, Huang, C. L., A Errigo., Y Yin., Lu, J., Ayala, M., Zhang, S.C. (2014). Modeling ALS with iPSCs reveals that mutant SOD1 misregulates neurofilament balance in motor neurons. *Cell. Stem Cell*. *14(6)*, 796–809. https://doi.org/10.1016/j.stem.2014.02.004

Clément, J-P., Al-Alwan, L., Glasgow, S.D., Stolow, A., Ding, Y., Melo, T.Q., Khayachi, A., Hellmund, M., Haag, R., Milnerwood, A.J., Grütter, P., Kennedy, T.E. (2022). Dendritic Polyglycerol Amine: An Enhanced Substrate to Support Long-Term Neural Cell Culture. ASN Neuro. Accepted for publication. DOI: 10.1177/17590914211073276.

Dasen, J. S., De Camilli, A., Wang, B., Tucker, P. W., Jessell, T. M. (2008). Hox repertoires for motor neuron diversity and connectivity gated by a single accessory factor. *FoxP*, *1*, *Cell 134*(2), 304–316. https://doi.org/10.1016/j.cell.2008.06.019

Dasen, J. S., Liu, J. P., Jessell, T. M. (2003). Motor neuron columnar fate imposed by sequential phases of Hox-c activity. *Nature*, *425*(6961), 926–933. https://doi.org/10.1038/nature02051

Devlin, A. C., Burr, K., Borooah, S., Foster, J. D., Cleary, E. M., Geti, I., Vallier, L., Shaw, C. E., Chandran, S., Miles, G. B. (2015). Human iPSC-derived motoneurons harbouring TARDBP or C9ORF72 ALS mutations are dysfunctional despite maintaining viability. *Nat. Commun*, *6*, 5999. https://doi.org/10.1038/ncomms6999

D'Orsi, B., Kilbride, S. M., Chen, G., Perez Alvarez, S., Bonner, H. P., Pfeiffer, S., Plesnila, N., Engel, T., Henshall, D. C., Dussmann, H., Prehn, J. H. (2015). Bax regulates neuronal Ca2 + homeostasis. *J. Neurosci*, *35*(4), 1706–1722. https://doi.org/10.1523/JNEUROSCI.2453-14.2015

Du, Z. W., Chen, H., Liu, H., Lu, J., Qian, K., Huang, C. L., Zhong, X., Fan, F., Zhang, S. C. (2015). Generation and expansion of highly pure motor neuron progenitors from human pluripotent stem cells. *Nat. Commun*, *6*, 6626. https://doi.org/10.1038/ncomms7626

Ebert, A.D., Yu, J., Rose, F. FJr, Mattis, V. B., Lorson, C. L., Thomson, J. A., & C. N Svendsen. (2009). Induced pluripotent stem cells from a spinal muscular atrophy patient. *Nature*, *457*(7227), 277–280. https://doi.org/10.1038/nature07677

Egawa, N., Kitaoka, S., Tsukita, K., Naitoh, M., Takahashi, K., Yamamoto, T., Adachi, F., Kondo, T., Okita, K., Asaka, I., Aoi, T., Watanabe, A., Yamada, Y., Morizane, A., Takahashi, J., Ayaki, T., Ito, H., Yoshikawa, K., Yamawaki, S.…& Inoue, H. (2012). Drug screening for ALS using patient-specific induced pluripotent stem cells. *Sci. Transl. Med*, *4*(145), 145ra104.

Frade, J. M., Barde, Y. A. (1999). Genetic evidence for cell death mediated by nerve growth factor and the neurotrophin receptor p75 in the developing mouse retina and spinal cord. *Development (Cambridge, England)*, *126*(4), 683–690. https://doi.org/10.1242/dev.126.4.683

Hellmund, M., Achazi, K., Neumann, F., Thota, B. N., Ma, N., Haag, R. (2015). Systematic adjustment of charge densities and size of polyglycerol amines reduces cytotoxic effects and enhances cellular uptake. *Biomaterials Science*, *3*(11), 1459–1465. https://doi.org/10.1039/C5BM00187K

Hellmund, M., Zhou, H., Samsonova, O., Welker, P., Kissel, T., Haag, R. (2014). Functionalized polyglycerol amine nanogels as nanocarriers for DNA. *Macromol. Biosci*, *14*(9), 1215–1221. https://doi.org/10.1002/mabi.201400144

Ho, R., Sances, S., Gowing, G., Amoroso, M. W., O'Rourke, J. G., Sahabian, A., Wichterle, H., Baloh, R. H., Sareen, D., Svendsen, C. N. (2016). ALS Disrupts spinal motor neuron maturation and aging pathways within gene co-expression networks. *Nat. Neurosci*, *19*(9), 1256–1267. https://doi.org/10.1038/nn.4345

Huang da, W., Sherman, B. T., Lempicki, R. A. (2009). Systematic and integrative analysis of large gene lists using DAVID bioinformatics resources. *Nat. Protoc*, *4*(1), 44–57. https://doi.org/10.1038/nprot.2008.211

Kanning, K. C., Kaplan, A., Henderson, C. E. (2010). Motor neuron diversity in development and disease. *Annu. Rev. Neurosci*, *33*, 409–440. https://doi.org/10.1146/annurev.neuro.051508.135722

Kharkar, P. M., Kiick, K. L., Kloxin, A. M. (2013). Designing degradable hydrogels for orthogonal control of cell microenvironments. *Chem. Soc. Rev*, *42*(17), 7335–7372. https://doi.org/10.1039/C3CS60040H

Kiskinis, E., Sandoe, J., Williams, L. A., Boulting, G. L., Moccia, R., Wainger, B. J., Han, S., Peng, T., Thams, S., Mikkilineni, S., Mellin, C., Merkle, F.T., Davis-Dusenbery, B.N., Ziller, M., Oakley, D., Ichida, J., Di Costanzo, S., Atwater, N., Maeder, M.L., …& Eggan, K. (2014). Pathways disrupted in human ALS motor neurons identified through genetic correction of mutant SOD1. *Cell. Stem Cell*, *14*, 781–795. https://doi.org/10.1016/j.stem.2014.03.004

Kuijlaars, J., Oyelami, T., Diels, A., Rohrbacher, J., Versweyveld, S., Meneghello, G., Tuefferd, M., Verstraelen, P., Detrez, J. R., Verschuuren, M., De Vos, W.H., Meert, T., Peeters, P.J., Cik, M., Nuydens, R., Brône, B., & Verheyen, A. (2016). Sustained synchronized neuronal network activity in a human astrocyte co-culture system. *Sci. Rep*, *6*, 36529. https://doi.org/10.1038/srep36529

Li, X. J., Du, Z. W., Zarnowska, E. D., Pankratz, M., Hansen, L. O., Pearce, R. A., Zhang, S. C. (2005). Specification of motoneurons from human embryonic stem cells. *Nat. Biotechnol*, *23*(2), 215–221. https://doi.org/10.1038/nbt1063

Luisier, R., Tyzack, G.E., Hall, C.E., Mitchell, J.S., Devine, H., Taha, D.M., Malik, B., Meyer, I., Greensmith, L., Newcombe, J., Ule, J., Luscombe, N.M., & Patani, R. (2018). Intron retention and nuclear loss of SFPQ are molecular hallmarks of ALS. *Nat. Commun*, *9*(1), 2010–2018-04373-8. https://doi.org/10.1038/s41467-018-04373-8

Lun, A. T., McCarthy, D. J., Marioni, J. C. (2016). A step-by-step workflow for low-level analysis of single-cell RNA-seq data with bioconductor. *F, 1000R. es*, *5*, 2122. doi: 10.12688/f1000research.9501.2.

Mertens, J., Paquola, A. C. M., Ku, M., Hatch, E., Bohnke, L., Ladjevardi, S., McGrath, S., Campbell, B., Lee, H., Herdy, J. R., Gonçalves, J.T., Toda, T., Kim, Y., Winkler, J., Yao, J., Hetzer, M.W., & Gage, F. H. (2015). Directly reprogrammed human neurons retain aging-associated transcriptomic signatures and reveal Age-related nucleocytoplasmic defects. *Cell. Stem Cell*, *17*(6), 705–718. https://doi.org/10.1016/j.stem.2015.09.001

Methot, L., Soubannier, V., Hermann, R., Campos, E., Li, S., Stifani, S. (2018). Nuclear factor-kappaB regulates multiple steps of gliogenesis in the developing murine cerebral cortex. *Glia*, *66*(12), 2659–2672. https://doi.org/10.1002/glia.23518

Miller, J. D., Ganat, Y. M., Kishinevsky, S., Bowman, R. L., Liu, B., Tu, E. Y., Mandal, P. K., Vera, E., Shim, J. W., Kriks, S., Taldone, T., Fusaki, N., Tomishima, M. J., Krainc, D., Milner, T. A., Rossi, D. J., & Studer, L. (2013). Human iPSC-based modeling of late-onset disease via progerin-induced aging. *Cell. Stem Cell*, *13*(6), 691–705. https://doi.org/10.1016/j.stem.2013.11.006

Naujock, M., Stanslowsky, N., Bufler, S., Naumann, M., Reinhardt, P., Sterneckert, J., Kefalakes, E., Kassebaum, C., Bursch, F., Lojewski, X., Storch, A., Frickenhaus, M., Boeckers, T. M., Putz, S., Demestre, M., Liebau, S., Klingenstein, M., Ludolph, A. C., Dengler, R., … & Petri, S. (2016). 4-Aminopyridine Induced activity rescues hypoexcitable motor neurons from amyotrophic lateral sclerosis patient-derived induced pluripotent stem cells. *Stem Cells (Dayton, Ohio)*, *34*(6), 1563–1575. https://doi.org/10.1002/stem.2354

Nijssen, J., Comley, L. H., Hedlund, E. (2017). Motor neuron vulnerability and resistance in amyotrophic lateral sclerosis. *Acta Neuropathologica*, *133*(6), 863–885. https://doi.org/10.1007/s00401-017-1708-8

Patani, R., Lewis, P. A., Trabzuni, D., Puddifoot, C. A., Wyllie, D. J., Walker, R., Smith, C., Hardingham, G. E., Weale, M., Hardy, J., Chandran, S., Ryten, M. (2012). Investigating the utility of human embryonic stem cell-derived neurons to model ageing and neurodegenerative disease using whole-genome gene expression and splicing analysis. *J. Neurochem*, *122*(4), 738–751. https://doi.org/10.1111/j.1471-4159.2012.07825.x

Qu, Q., Li, D., Louis, K. R., Li, X., Yang, H., Sun, Q., Crandall, S. R., Tsang, S., Zhou, J., Cox, C. L., Cheng, J., Wang, F. (2014). High-efficiency motor neuron differentiation from human pluripotent stem cells and the function of islet-1. *Nat. Commun*, *5*, 3449. https://doi.org/10.1038/ncomms4449

Sareen, D., O'Rourke, J. G., Meera, P., Muhammad, A. K., Grant, S., Simpkinson, M., Bell, S., Carmona, S., Ornelas, L., Sahabian, A., Gendron, T., Petrucelli, L., Baughn, M., Ravits, J., Harms, M. B., Rigo, F., Bennett, C. F., Otis, T. S., Svendsen, C. N., & Baloh, R. H. (2013). Targeting RNA foci in iPSC-derived motor neurons from ALS patients with a C9ORF72 repeat expansion. *Sci. Transl. Med*, *5*(208), 208ra149. https://doi.org/10.1126/scitranslmed.3007529

Schmidt, S., Lilienkampf, A., Bradley, M. (2018). New substrates for stem cell control. *Philos. Trans. R. Soc. Lond. B. Biol. Sci*, *373(1750)*(1750), 10. https://doi.org/10.1098/rstb.2017.0223

Stegle, O., Teichmann, S. A., Marioni, J. C. (2015). Computational and analytical challenges in single-cell transcriptomics. *Nat. Rev. Genet*, *16*(3), 133–145. https://doi.org/10.1038/nrg3833

Taga, A., Dastgheyb, R., Habela, C., Joseph, J., Richard, J. P., Gross, S. K., Lauria, G., Lee, G., Haughey, N., Maragakis, N. J. (2019). Role of human-induced pluripotent stem cell-derived spinal cord astrocytes in the functional maturation of motor neurons in a multielectrode array system. *Stem Cells Transl. Med*, *8*(12), 1272–1285. https://doi.org/10.1002/sctm.19-0147

Thaler, J., Harrison, K., Sharma, K., Lettieri, K., Kehrl, J., Pfaff, S. L. (1999). Active suppression of interneuron programs within developing motor neurons revealed by analysis of homeodomain factor HB9. *Neuron*, *23*(4), 675–687. doi: 10.1016/s0896-6273(01)80027-1.

Thaler, J. P., Lee, S. K., Jurata, L. W., Gill, G. N., Pfaff, S. L. (2002). LIM Factor Lhx3 contributes to the specification of motor neuron and interneuron identity through cell-type-specific protein-protein interactions. *Cell*, *110*(2), 237–249. https://doi.org/10.1016/S0092-8674(02)00823-1

Thiry, L., Hamel, R., Pluchino, S., Durcan, T., Stifani, S. (2020). Characterization of human iPSC-derived spinal motor neurons by single-cell RNA sequencing. *Neuroscience*, *450*, 57–70. https://doi.org/10.1016/j.neuroscience.2020.04.041

Tsang, Y. M., Chiong, F., Kuznetsov, D., Kasarskis, E., Geula, C. (2000). Motor neurons are rich in non-phosphorylated neurofilaments: Cross-species comparison and alterations in ALS. *Brain Research*, *861*(1), 45–58. https://doi.org/10.1016/S0006-8993(00)01954-5

Wainger, B. J., Kiskinis, E., Mellin, C., Wiskow, O., Han, S. S., Sandoe, J., Perez, N. P., Williams, L. A., Lee, S., Boulting, G., Berry, J. D., Brown, R. H. Jr, Cudkowicz, M. E., Bean, B. P., Eggan, K., & Woolf, C. J. (2014). Intrinsic membrane hyperexcitability of amyotrophic lateral sclerosis patient-derived motor neurons. *Cell. Rep*, *7*(1), 1–11. https://doi.org/10.1016/j.celrep.2014.03.019

Wang, H., Heilshorn, S. C. (2015). Adaptable hydrogel networks with reversible linkages for tissue engineering. *Advanced Materials*, *27*(25), 3717–3736.

Wei, M. C., Zong, W. X., Cheng, E. H., Lindsten, T., Panoutsakopoulou, V., Ross, A. J., Roth, K. A., MacGregor, G. R., Thompson, C. B., Korsmeyer, S. J. (2001). Proapoptotic BAX and BAK: A requisite gateway to mitochondrial dysfunction and death. *Science (New York, N.Y.)*, *292*(5517), 727–730. doi: 10.1126/science.1059108.

William, C. M., Tanabe, Y., Jessell, T. M. (2003). Regulation of motor neuron subtype identity by repressor activity of Mnx class homeodomain proteins. *Development (Cambridge, England)*, *130*(8), 1523–1536. https://doi.org/10.1242/dev.00358

Zhang, K., Donnelly, C. J., Haeusler, A. R., Grima, J. C., Machamer, J. B., Steinwald, P., Daley, E. L., Miller, S. J., Cunningham, K. M., Vidensky, S., … (2015). The C9orf72 repeat expansion disrupts nucleocytoplasmic transport. *Nature, 525*(7567), 56–61. https://doi.org/10.1038/nature14973